



Evaluation of drug delivery profiles in geometric three-layered tablets with various mechanical properties, *in vitro*–*in vivo* drug release, and Raman imaging

Du Hyung Choi^a, Ki Hyun Kim^b, Jun Sang Park^c, Seong Hoon Jeong^{b,*}, Kinam Park^d

^a College of Pharmacy, Pusan National University, Busan 609-735, Republic of Korea

^b College of Pharmacy, Dongguk University-Seoul, Goyang, Gyeonggi 410-820, Republic of Korea

^c GL PharmTech Corp., Seongnam, Gyeonggi 462-807, Republic of Korea

^d Department of Pharmaceutics and Biomedical Engineering, Purdue University, West Lafayette 47907, USA

ARTICLE INFO

Article history:

Received 6 May 2013

Accepted 26 August 2013

Available online 12 September 2013

Keywords:

Geometric tablet

Raman imaging

Multi-layered tablet

Mechanical properties

Rheology

Diffusion

ABSTRACT

Even though various multi-layered tablets have been developed for sustained release formulations, evaluations of mechanical properties during dissolution with drug release and imaging in the tablets have been limited. A novel geometric system consisting of an inner immediate release layer and two extended release barrier layers with swellable hydrophilic polymers was suggested as a once-a-day formulation. To evaluate drug release mechanisms with geometric properties, various mechanical characteristics during swelling were investigated to comprehend the relationship among *in vitro* drug release, human pharmacokinetics, and geometric characteristics. Imaging of drug movement was also studied in real-time using Raman spectroscopy. Drug delivery in the tablets might be divided into three processes through the geometric properties. When exposed to aqueous environments, the drug in the mid-layer was released until wrapped by the swollen barrier layers. Then, the drug in the mid-layer was mainly delivered to the barrier layers and a small amount of the drug was delivered to the contact region of the swollen barrier layers. Finally, the delivered drug to the barrier layers was consistently released out in response to the characteristics of the polymer of the barrier layers. Using Raman spectroscopy, these processes were confirmed in real-time analysis. Moreover, *in vitro* drug release profiles and human pharmacokinetics showed consistent results suggesting that drug release might be dependent on the various geometric properties and be modified consistently during the formulation development.

© 2013 Elsevier B.V. All rights reserved.

1. Introduction

Oral solid drug dosage formulations have been regarded as the most convenient and commonly used method of drug administration due to their numerous advantages, such as ease of drug administration, high patient compliance, least aseptic constraints, and flexibility for the design of the dosage forms [1]. The advantages and the various types of dosage forms have been developed continuously and they are classified according to their release profiles, which include immediate release, modified release, delayed release, extended release, and sustained release. Immediate release forms dissolve above the small intestine with the intention of fast dissolution or absorption of drugs. Both delayed and extended release forms belong to the modified release class. Delayed release forms have a special release profile dissolved at the target area. Extended release forms have been developed to optimize the

therapeutic efficacy of drugs by providing constant release over the entire dosing interval and increase patient convenience by reducing the frequency of drug administration [2].

Generally, modified systems should ideally exhibit zero-order drug release kinetics in which a constant amount of drug is released over an extended period of time [3,4]. Studies have been conducted attempting to develop systems with zero-order drug release [5–9]. A matrix type, in which the drug is uniformly dissolved or dispersed, is the most common one [10,11]. Hydrophilic polymers are mainly incorporated for the matrix formulation as they provide a typical time dependent dissolution curve of drug release [12–15]. However, the drug release of the hydrophilic matrix follows near first-order diffusion for the initial stage with a high release rate, owing to the drug existence at the surface of the matrix (burst effect). This undesirable effect may have negative therapeutic effects. Moreover, this phenomenon significantly increases the contact region of the systems with aqueous medium, so the physical properties of the hydrophilic matrix such as swelling, water absorption, mass loss, and gel hardness are changed with the absorption of the aqueous medium.

To overcome the undesirable influence of the hydrophilic matrix, geometric matrix tablets have been investigated to achieve zero-

* Corresponding author at: College of Pharmacy, Dongguk University-Seoul, Donggukro 32, Ilsandonggu, Goyang, Gyeonggi 410-820, Republic of Korea. Tel.: +82 31 961 5225.
E-mail address: shjeong@dongguk.edu (S.H. Jeong).

order kinetics as the tablets induce a constant surface area for drug release [16–19]. Various geometric matrix tablets have been suggested to achieve a constant release rate (zero-order kinetics). The multi-layered matrix tablets are one of the various techniques. They are composed of a matrix core containing the drug and one or more barriers (control layers). The control layers modulate the interaction of the drug with an aqueous medium by limiting the surface available for the solute release and controlling the solvent penetration rate [20,21]. In other words, the control layers organized mainly with hydrophilic polymers such as hydroxypropyl methyl cellulose and polyethylene oxide perform swelling and erosion processes during contact with the aqueous medium. Drug release can be controlled by diffusion, path-length and the area available for drug release. Therefore, the mechanical properties of the control layers can play an important role for the successful development of formulations [2].

The mechanical properties of the control layers are dependent on various factors that include drug solubility, drug-to-polymer ratio, polymer viscosity, particle size of the drug and polymer, and the water-soluble excipient ratio [22]. For these reasons, drug release tests of multi-layered matrix tablets should be conducted with the evaluations of mechanical properties as well. Moreover, due to the characteristics of geometries, it is important to study the pathways of drug movement in the system. The macroscopic drug movements can be evaluated by a dissolution test, because the drug movement in the system is not easy and is quite limited. In this study, a spectroscopic method was utilized for real-time analysis of drug distribution in the system.

Imaging techniques using spectroscopic methods provide unique information about complicated drug delivery processes and pharmaceutical process analytical techniques. Typical examples are infrared and Raman spectroscopy. Infrared spectroscopy has good sensitivity to moisture and has been utilized for pharmaceutical applications such as end-point determination in blending and process controls (granulation, drying, and coating) [23–26]. However, the infrared spectrum of water is too intense to be used in aqueous systems. On the other hand, the Raman spectrum of water is weak so that data collection is possible in an aqueous environment. Raman spectroscopy investigates the same range of energies as infrared with different applications. In the case of infrared transition, dipole moment, is associated with a molecular vibration that decides the intensity of the transition. However, Raman scattering relies on the subsequent scattering of a photon from dipole [27,28]. The electronic structure of water is the σ -bond, which has a strong dipole moment. Therefore, the electrons of water are not polarized with weak Raman scattering. On the other hand, many active pharmaceutical ingredients (APIs) have π -electrons in molecules providing strong Raman scattering as they are polarized [29]. Due to the good sensitivity for APIs and the insensitivity for water, Raman spectroscopy may be utilized to investigate drug movement in dosage forms during dissolution.

A novel geometric system consisting of an inner immediate release layer and two extended release barrier layers with swellable hydrophilic polymers has been suggested as a once-a-day formulation [30]. In this system, the aqueous medium rapidly penetrates to the mid-layer of water-soluble excipients and the two barrier layers swell to wrap the lateral side of the mid-layer. After oral administration, tablet hydration might occur quickly and the hydrated tablet might reach the colon where water is quite limited. Therefore, it was assumed that the hydrated state of the tablet might induce continuous drug release even in the colon. To confirm these assumptions, various mechanical properties of the geometric system were investigated especially to comprehend the relationship among *in vitro* drug release, human pharmacokinetics, and geometric characteristics. Moreover, imaging of drug movement in the system was performed in real-time using Raman spectroscopy for better understanding of drug release profiles in the geometric multi-layered system.

2. Materials and methods

2.1. Materials

The model drug, tamsulosin HCl dihydrate, was purchased from Cadila Healthcare (Gujarat, India). As a hydrophilic polymer in the three-layered tablets, polyethylene oxide (PEO; Polyox WSR-303) of average molecular weight 7×10^6 grades was used and obtained from Dow Chemical (Midland, MI, USA). Polyethylene glycol 6000 (Macrogol 6000) was purchased from Sanyo Chemical Industries (Ibaraki, Japan). Pearlitol 160C was obtained from Roquette Korea (Seoul, South Korea). Sodium chloride (NaCl) was purchased from Sigma-Aldrich (St. Louis, MO, USA). The NaCl was milled with a mortar and pestle and sieved with a US standard sieve #200. Magnesium stearate was purchased from Faci Asia (Jurong Island, Singapore). All other reagents were of analytical or high-performance liquid chromatography (HPLC) grade and used as received.

2.2. Preparation of three-layered tablets

Table 1 summarizes the formulation components of the geometric three-layered tablets. The batch size was selected to be 500-tablets. Before the mixing process, all materials were passed through a #20 mesh sieve to remove any aggregates. For the preparation of the mid-layer, the model drug was mixed manually with the excipients except magnesium stearate with a mortar and pestle and then blended with magnesium stearate for 5 min. The component of the barrier layer was blended with magnesium stearate. Exact amount of each layer was loaded one-by-one into a die and compressed on a hydraulic laboratory press (Carver Press, Wabash, IN, USA) using place-face punches with a diameter of 9.0 mm. The compression pressure was 10.0 mPa.

2.3. Evaluation of water uptake and mass loss

The degree of water uptake was calculated when test tablets were immersed in 500 mL of dissolution medium (0.05 M phosphate buffer, pH 6.8) at 37 °C and stirred with a magnetic bar operating at 250 rpm. The test tablets were removed from the medium at predetermined time intervals (30, 60, 90, 120, 150, 180, 240, and 300 min), blotted with absorbent tissue to remove any excess dissolution medium on the surface, and the weight of the swollen tablets was measured. The degree of water uptake was calculated using the following equation [31]:

$$\text{Water uptake (\%)} = \left(\frac{W_2 - W_1}{W_1} \right) \times 100 \quad (1)$$

where, W_1 is the initial weight of the dry tablet and W_2 is the weight of the hydrated tablet. Mass loss values were calculated using the same tablets. After weighing, the hydrated tablet was dried in an oven at 60 °C until a constant weight was achieved and the remaining dry

Table 1
Formulation composition of the geometric three-layered tablet.

Layer components		Weight (mg)/tablet	Percentage (%)
Upper barrier layer	Polyox WSR 303	89.50	37.2
	Magnesium stearate	0.50	0.2
Mid-layer	Tamsulosin HCl	0.40	0.2
	Pearlitol 160C	30.00	12.5
	Macrogol 6000	20.00	8.3
	NaCl	9.60	4.0
	Magnesium stearate	0.30	0.1
Lower barrier layer	Polyox WSR 303	89.50	37.2
	Magnesium stearate	0.50	0.2

weight, W_3 , was obtained. Percent (%) mass loss (erosion) was calculated according to the following equation [31]:

$$\text{Mass loss (\%)} = \left(\frac{W_1 - W_3}{W_1} \right) \times 100. \quad (2)$$

2.4. Mechanical properties of swollen three-layered tablets

Swelling properties and mechanical gel strength of the hydrated tablets were evaluated using a texture analyzer. The tablets were placed in a beaker under the same conditions as explained in the water uptake and mass loss evaluations. The hydrated tablets were removed from the medium at predetermined time intervals, patted lightly with tissue paper, and subjected to textural profiling to determine the swelling profiles, movement of erosion and swelling fronts, and mechanical gel strength [32,33]. All measurements were carried out in triplicate for each time point. Analysis of textural profiles was performed using a TAXT express texture analyzer (Stable Micro Systems, Godalming, UK) equipped with a 5 kg load cell and Texture Expert software. The textural profiles were monitored using the force–displacement properties associated with the penetration of a 1.5 mm round-tipped probe into the swollen tablets [34]. When a trigger force reached 0.001 N, the signal began to be recorded and the probe was advanced into the sample at a test speed of 0.1 mm/s until the maximum force of 60 N was reached. The swelling profiles were determined by measuring the total probe displacement value recorded and observing the textural profiles. The axial swelling was calculated according to the following equation [31]:

$$\text{Axial swelling (\%)} = \left(\frac{T_2 - T_1}{T_1} \right) \times 100 \quad (3)$$

where, T_1 is the original thickness and T_2 is the swollen thickness of the test tablets. Total work of penetration (W_T), which is a measure of gel strength and resistance to probe penetration, was also determined from the textural profiles. F is the force applied and D is the distance traveled, according to Eq. (4).

$$\text{Total work of penetration } (W_T) = \int FdD \quad (4)$$

2.5. Rheological properties of the barrier layer

Rheological properties of the barrier layers were measured using an Advanced Rheometric Expansion system (ARES; Rheometric Scientific, Piscataway, NJ, USA) equipped with a parallel-plate fixture, having a radius of 12.5 mm and a gap size of 2.7 mm. The barrier layer tablets were prepared separately for this study. Granules of the barrier layer were put in the die, and then compressed on a single-punch hydraulic laboratory press using plane-face punches with a diameter of 9.0 mm. The barrier layer tablets were placed in a beaker under conditions identical to those described for the water uptake and mass loss evaluations. The hydrated samples were removed at predetermined time intervals and patted lightly with tissue paper. Before loading the sample, two plates were covered with sandpaper to get rid of a wall slippage between the test material and the plates. The frequency-sweep tests in the small amplitude oscillatory shear flow fields were carried out over an angular frequency range from 0.01 to 100 rad/s with a logarithmically increasing scale at a constant strain amplitude of 0.1% (from strain-sweep tests, this strain value was confirmed to lie within the linear viscoelastic region for the sample).

2.6. Drug diffusion of the barrier layer

The preliminary diffusion study of the hydrophilic polymers using side-by-side diffusion cells gave so much variation due to the inconsistent erosion after swelling. Therefore, a special experimental device was designed. Fig. 1 shows a schematic view of the diffusion test using side-by-side cells with polyacrylate plates and a cellulose acetate membrane. The barrier layer tablet was prepared with a single-punch hydraulic laboratory press, identical to those described above for the rheology evaluation.

For the pre-gelling step, the barrier layer tablets were inserted into the housing made of polyacrylate (15 × 20 mm, 9 mm hole) and both sides of the central part were supported by a cellulose acetate membrane (0.20 μm pore size). The pre-gelling device was tied tightly with rubber bands as shown in Fig. 1a. The barrier layer tablets were immersed in 500 mL of dissolution medium (50 mM phosphate buffer, pH 6.8, 37 °C) and stirred with a magnetic bar (250 rpm) to gelation for 5 h. After gelling, the two polyacrylate plates located on the outside of the central part were removed carefully; and the swollen barrier layer tablet, wrapped on both sides by the membrane filters, was transferred to the side-by-side diffusion cells (Fig. 1b and c). The donor cell was filled with 4 mL of the drug solution (500 μg/mL in 50 mM pH 6.8 phosphate buffer) and the receptor cell was filled with 4 mL of the same buffer. Samples were withdrawn from the receptor cell at predetermined time intervals and the fresh buffer of the same volume was compensated. The acquired sample was centrifuged for 30 min and then the supernatant was analyzed using the HPLC system. To achieve consistent diffusion rates, the barrier layer tablet needs to get to a steady-state at the initial stage. When the steady-state portion of the line is extrapolated to the time axis, the point of intersection is known as the lag time (t_L). This is the time required for a drug to establish a uniform concentration gradient within the barrier layer tablet [35,36]. The lag time is given by

$$t_L = \frac{h^2}{6D} \quad (5)$$

where, t_L , D , and h are lag time, diffusion coefficient, and tablet thickness of the swollen barrier layer, respectively.

2.7. Drug release test

Drug release tests were carried out according to the USP 27 Apparatus 2 guidelines (paddle method) (Varian 705 DS; Varian, Cary, NC, USA) with 900 mL of dissolution medium maintained at 37 ± 0.5 °C and a paddle speed of 100 rpm. Each tablet was enclosed in a stationary basket to prevent the tablet from floating on the surface of the release medium or sticking to the inner surface of dissolution vessels ($n = 4$). The dissolution medium was simulated gastric fluid (pH 1.2) for the first 2 h and then was exchanged with simulated intestinal fluid (SIF; pH 6.8, 50 mM phosphate buffer) from 2 to 24 h without any enzymes. Samples were withdrawn at predetermined time intervals and analyzed for drug content using an Agilent 1100 Series HPLC system (Agilent Technologies, Santa Clara, CA, USA) with UV detection at a wavelength of 225 nm. A Kromasil C18, 5 μm (4.6 × 250 mm) (Sigma-Aldrich) column was used and maintained at 40 °C. The mobile phase was a mixture of aqueous buffer (pH 3.2, 35 mM phosphate buffer) and acetonitrile in a volume ratio of 70:30. The flow rate was 1.0 mL/min and the injection volume was 20 μL. The cumulative percentage (%) of drug released was calculated and the results were presented as the mean value of at least four tablets.

2.8. Imaging of drug migration with Raman spectroscopy

Due to its good sensitivity for the model drug and insensitivity for water, Raman spectroscopy was utilized to monitor drug migration in

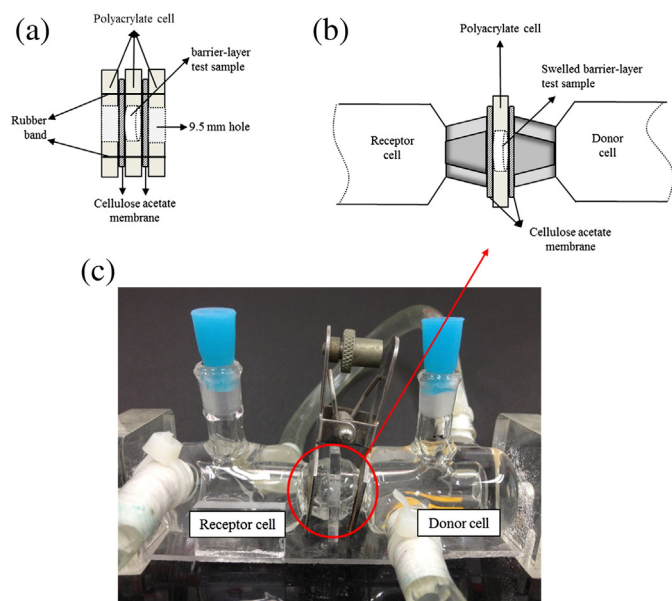


Fig. 1. Schematic view of the modified diffusion test using side-by-side diffusion cells with polyacrylate plates and a cellulose acetate membrane. (a) Depiction of the in-house pre-gelling device. (b) Swollen barrier layer positioned between the diffusion cells. (c) Photograph of diffusion test equipped with the swollen barrier layer.

the system during hydration and drug release. The drug in the system can be dissolved in the release medium and migrate with the movement of the medium. To monitor the pathways of the drug migration in the system, three points of a cross section in a sample were imaged: a) the area neighboring the surface in the swollen barrier layer, b) the interface between the mid-layer and the barrier layer, and c) the interface between the mid-layer and the contact region of the swollen barrier layer. Test tablets were placed in a beaker under the conditions identical to those described for water uptake and erosion evaluations. The hydrated tablets were removed at predetermined time intervals and patted lightly with tissue paper. The samples were cut vertically giving clear-cut cross sections.

Raman spectroscopy utilized the Raman RXN1™ Systems (Kaiser Optical Systems, MI, USA). Using a set of lenses, the instrument was collimated to form a circular illumination area with a diameter of 6 mm to cover a large sampling area. This wide area illumination scheme reduces the errors due to focusing and improves the reproducibility of sampling [37,38]. A holographic transmission grating was used to disperse the collected backscatter from the optical fibers and signal integration was performed using an air-cooled CCD detector. Data collection and data transfer were automated using the Matlab® software package, version 6.5 (The MathWorks, Natick, MA, USA) and the collected data was imaged by HoloMap™ (Kaiser Optical Systems).

2.9. Pharmacokinetic study in humans

The experiments for the pharmacokinetic evaluations were approved by the institutional review board of Ajou University Hospital (Suwon, Gyeonggi, Korea). All subjects were enrolled in this study after performing a medical history assessment, physical examination, and standard laboratory testing. As part of the laboratory analyses, blood analyses included hemoglobin, hematocrit, red blood cell (RBC) count, white blood cell (WBC) count, platelet count, differential counting of WBC, total protein, albumin, serum glutamic oxaloacetic transaminase (sGOT), serum glutamic pyruvic transaminase (sGPT), alkaline phosphatase, total bilirubin, cholesterol, creatinine, blood urea nitrogen, and (fasting) glucose. Laboratory analyses also included examination of urine for specific gravity, color, pH, sugar, albumin, bilirubin, RBC, WBC and cast. All of the participants signed a written consent

form after they had been informed of the nature and details of the study in accordance with the revised Declaration of Helsinki and the Good Clinical Practice guidelines (KGCP) (KFDA 2009). After an overnight fast (12 h), volunteers were given test tablets with 240 mL of water. The subjects were hospitalized (Ajou University Hospital) at 10:00 p.m. on the evening prior to the study and fasted overnight for 4 h after drug administration. About 7.0 mL of blood samples were collected from each volunteer using a catheter inserted into the median cubital vein into heparinized tubes before (0 h) and at 1, 2, 3, 4, 5, 6, 7, 8, 9, 10, 12, 24, and 48 h after dosing. The plasma was separated by centrifugation at 3000 rpm for 7 min and kept frozen at -70°C until analysis.

Standard and quality control samples were calibrated and prepared as follows. A stock solution of tamsulosin was prepared in 50% acetonitrile at 918 $\mu\text{g}/\text{mL}$. This stock solution was further diluted with 50% acetonitrile to obtain tamsulosin calibration standard solutions with concentrations of 2, 4, 10, 40, 100, 200 and 400 ng/mL. Plasma calibration at concentrations of 0.1, 0.2, 0.5, 2, 5, 10, and 20 ng/mL were obtained by the addition of stock solution to blank plasma. Quality control (QC) samples (0.3, 3, and 15 ng/mL) were also similarly prepared. To prepare stock solutions (918 $\mu\text{g}/\text{mL}$) of internal standard (IS), 1 mg of tamsulosin- d_4 was dissolved in 1 mL of 50% acetonitrile and diluted further to the final concentration of 30 ng/mL. After thawing the samples at room temperature, an aliquot of each sample (200 μL) was pipetted into a polypropylene tube and 20 μL of IS working solution (30 $\mu\text{g}/\text{mL}$) was added. After vortexing briefly, 1.5 mL of the organic solvent (methyl *tert*-butyl ether) was added to each sample, shaken for 20 min, and then centrifuged for 5 min at 13,000 rpm. The upper organic layer was transferred to another tube and evaporated to dryness in a MG-2100 (Eyela, Tokyo, Japan) evaporation system at 50°C . The residue was resolved in 300 μL of acetonitrile (50%, v/v) and then injected (5 μL) onto the liquid chromatography-tandem mass spectrometry (LC-MS/MS) system.

A Shiseido nanospace SI-2 HPLC system (Shiseido, Tokyo, Japan) and an API 4000 mass spectrometer (Applied Biosystems/MDS SCIEX, Concord, ON, Canada) equipped with a Turboionspray® or™ ionization source operating in electrospray ionization (ESI) positive ion mode were used for the LC-MS/MS analysis. Two channels of a positive ion MRM mode were used to detect tamsulosin and the IS. The most abundant product ions of the compounds were at m/z 228.1 from the precursor ion m/z 409.3 of tamsulosin and at m/z 228.1 from the m/z 413.2 of the IS. Data acquisition was performed with Analyst 1.4.1 software (AB SCIEX, Toronto, ON, Canada). The analytical column used was Hypersil Gold (150 \times 2.1 mm i.d. 5 μm , Thermo Scientific, Hudson, NH, USA). The mobile phase consisting of 50% methanol and 50% 5 mM ammonium formate buffer was filtered through a 0.2 μm filter and degassed before use. A flow rate of 0.25 mL/min was used for sample analysis. The temperatures of the autosampler and column oven were 10°C and 40°C , respectively.

3. Results and discussion

3.1. Evaluation of water uptake and mass loss of the three-layered tablets

The extent of water uptake might be dependent on many factors including the ratio among excipients, geometrics of a tablet, and compression pressure. Moreover, drug solubility may influence water penetration into the system and also the water uptake process [39–41]. The geometric characteristics of this system are intended to control drug release for once-a-day use by designing induced “self-dissolution” as the system moves down the lower gastrointestinal (GI) tract, where the dissolution medium is limited. For this purpose, the hydrophilic polymer was used to absorb and maintain water for a longer period of time in the upper GI tract, where dissolution medium is abundant. The drug can move down with the absorbed aqueous medium and, hence, the

evaluations of the water uptake and mass loss might be important to understand drug migration and release profiles in the system.

The water uptake and mass loss evaluations were performed by comparing the weight of the swollen and the dried tablets. As shown in Fig. 2a, after 5 h of the experiment, the test tablets had about 8-fold their initial weight and consistently absorbed the aqueous medium. The barrier layers seemed to absorb the aqueous medium steadily to the maximum capacity of the polymer. Moreover, it might be possible that, compared to simple matrix formulations, continuous water absorption of the system might be affected by the presence of the mid-layer. The mid-layer was composed of water-soluble excipients. During the initial stage of the water uptake, the lateral surface of the mid-layer was eroded before it was wrapped or covered by the swollen barrier layers. The eroded area of the mid-layer might be filled with the aqueous medium, which may affect the mid-layer's erosion and the drug migration.

The mass loss was sharply increased up to 10% in 30 min and about a 35% loss occurred after 5 h (Fig. 2b). As already suggested, the initial mid-layer's erosion affected the initial mass loss before the complete wrapping of the mid-layer by the barrier layers. The mass loss was increased gradually from 0.5 h to 2.5 h suggesting a minimal mass loss from the mid-layer during this time. The swollen barrier layers fully wrapped the mid-layer while swelling continuously. However, the erosion properties were more significant than the swelling after 2.5 h so the mass loss increased significantly. After 2.5 h, this system, totally surrounded by the swollen barrier layers, was eroded on the outer surface. These swelling/erosion properties affected the overall thickness of the tablets, which might influence the drug release kinetics due to the change of the distance to move [42].

3.2. Evaluation of swelling properties and penetration work with a texture analyzer

Drug migration of the system is dependent on the pathways of the dissolution medium similar to the hydrophilic matrix system. Hydrophilic polymers exposed to an aqueous medium swell first instead of disintegrating because of the rapid gel formation. When the aqueous medium contacts the polymers, the size of the polymer molecules increases as the polymer passes from the crystalline state to the gel layer. From this gel layer, the aqueous medium enters further to the inside of the system and the dissolved drug moves to the outside of the system. The continuous supply of aqueous medium causes an increase of the gel thickness and the system erodes steadily. At the same time, the polymer chains gradually slacken until erosion begins [22].

According to the interactions between drug migration and the polymer physical properties, swelling profiles and total penetration work of the probe were evaluated by the texture analyzer. Textural profiles were used to study the dynamics of gel strength and movement of gel boundaries. This helps the understanding of the water/drug movement in the test tablet. Fig. 3a shows the resulting profiles of the test tablet obtained at predetermined time intervals. The thickness was gradually increased for 3 h. However, it was significantly decreased after 4 h due to the barrier layer's erosion and disintegration of the mid-layer. The resistance force peak on the mid-layer appeared at 1 h and 2 h. However, it did not appear after 3 h, suggesting that the mid-layer was completely dissolved by 3 h [31]. Therefore, the disintegrated drug in the mid-layer may have freely moved to the barrier layer or the contact regions of the swollen barrier layer.

As shown in Fig. 3b, axial swelling properties were increased up to 150% for 3 h and then decreased to 97% until 6 h. When test tablets were immersed, the physical interactions, including hydrogen bonding between the barrier layer's polymers and water, occurred strongly at the initial stage. At this time, the polymer chains started to unfold and the size of the polymer molecules increased. Therefore, the thickness of the system increased as more aqueous medium entered the system for 3 h. However, the polymers on the surface of the system, which

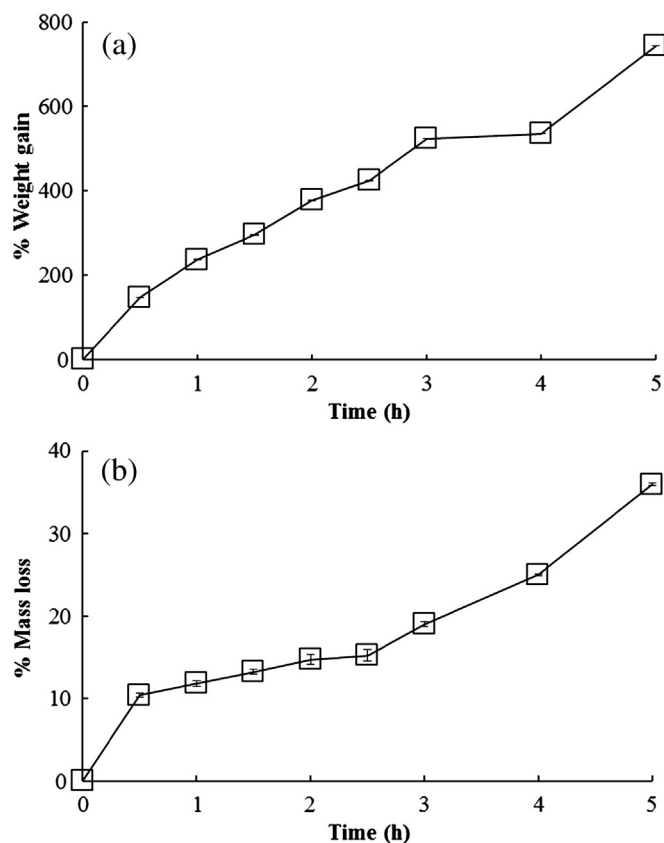


Fig. 2. In vitro evaluation of (a) weight gain (%; water uptake) and (b) mass loss (%) of the three-layered tablets ($n = 4$).

became hydrated earlier than the others, gradually relaxed until they began eroding. The axial swelling properties decreased after 3 h. Relaxation of the polymer chains represented the total penetration work (Fig. 3c). The interaction force of the polymer chains was gradually decreased from the initial stage. As water penetrated, the polymer might change from a crystalline state to a rubbery state. In this case, the binding force between the polymers was reduced. The force of penetration was mainly influenced by the binding forces between the barrier layer's polymer and the mid-layer's disintegration. Before the mid-layer was

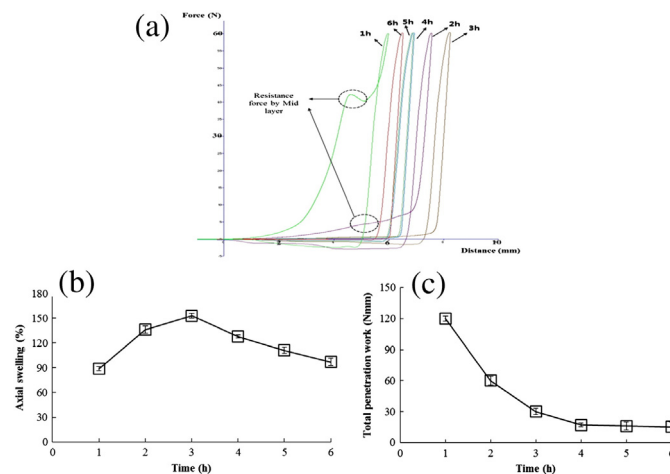


Fig. 3. Evaluation of the gelling properties of the swollen tablets ($n = 4$). (a) Dynamics of gel strength and movement of gel boundaries with force–displacement properties of the swollen tablets, (b) axial swelling percent profiles of tablets, and (c) representative total penetration work profiles.

disintegrated, the total penetration work was influenced by the barrier layer's gel-forming/non-gel-forming and the mid-layer's hardness. However, the total penetration work was mainly influenced by the extent of the barrier layer's gel formation. The total penetration work was sharply decreased by 3 h. The mid-layer might have disintegrated and the barrier layer's polymer may have continuously formed a gel by 3 h, drastically changing the force of penetration. As the binding force between the polymers was continuously reduced after 3 h, erosion gradually began. Erosion affected the thickness of the tablets and the interaction between the polymers. Therefore, the force and the distance of penetration were decreased after 3 h. In other words, the total penetration work was decreased along with erosion progress after 3 h.

3.3. Rheological properties of the barrier layer

Solid-gel transition is an important physical property in a system involving a hydrophilic polymer. When the solid form of the hydrophilic polymer is exposed to an aqueous medium, a solid-gel transition occurs and a drug can move through the gel core [43–45]. Especially, the visco-elastic properties might be an important factor as the system needs to maintain geometric integrity while the drug is released until moving to the large intestine [46].

The frequency dependencies of the elastic modulus (the storage modulus: G') and the viscous modulus (the loss modulus: G'') for the barrier-layer are shown in Fig. 4. The general trend emerging at almost predetermined time points was that G' is much larger than G'' , suggesting that the elastic response dominates, which is typical for gel materials. However, as indicated in the circles of Fig. 4, G'' is larger than G' between 10^{-2} rad/s and 10^{-1} rad/s after 3 h. It can be suggested that the barrier layer is in contact with the aqueous medium formed gel. This change progressed with additional water absorption, so the rheological properties of the hydrated barrier layer displayed the elastic modulus at the time points. However, the erosion of the barrier layer began as continuous gelation progressed. Generally, the

hydrophilic polymer is beginning to be eroded from the outer portion of the gel.

As the gel layer gradually disappeared, the rheological properties of the barrier layers were changed in some degree. Therefore, the viscous modulus was larger than the elastic modulus at specific ranges (between 10^{-2} rad/s and 10^{-1} rad/s) after 3 h. Moreover, as gelation progressed continuously, the elastic modulus G' and the viscous modulus G'' were simultaneously decreased along with the continuous progress of gelation (Fig. 5).

3.4. Diffusion of the barrier layer

Diffusive drug transfer is important for many pharmaceutical applications using hydrophilic polymers. Generally, drug release through a hydrated polymer involves processes of drug diffusion through the gel layer formed by the swelling of the polymer chains [47]. The swelling is a result of the entry of water, which produces the swelling of the polymer or the drug dissolution [48,49]. Due to the geometric properties of the tablets, it was important to evaluate the diffusion profiles of the barrier layer to understand the drug migration.

As shown in Fig. 6, the drug diffusion profile of the barrier layer showed a steady state after 8 h. A steady state can be described in terms of Fick's second law. In the experiment, lag time and the diffusion coefficient were 8.29 h and $1.93 \text{ mm}^2/\text{h}$, respectively. Drug release could be sufficiently delayed through the barrier layer. Owing to the geometric properties of the test tablets, the initial drug release was dependent on the coverage of the mid-layer by the swollen barrier layer. After the mid-layer was wrapped, the drug in the mid-layer moved to the barrier layer, and the contact region of the swollen barrier layers suggested that the drug release was controlled by the diffusion at the barrier layer. However, the actual drug release kinetics may be faster than the assumption because the test tablet's erosion increased as more water penetrated. The thickness of the swollen barrier layer was steadily reduced as erosion of hydrophilic polymer began.

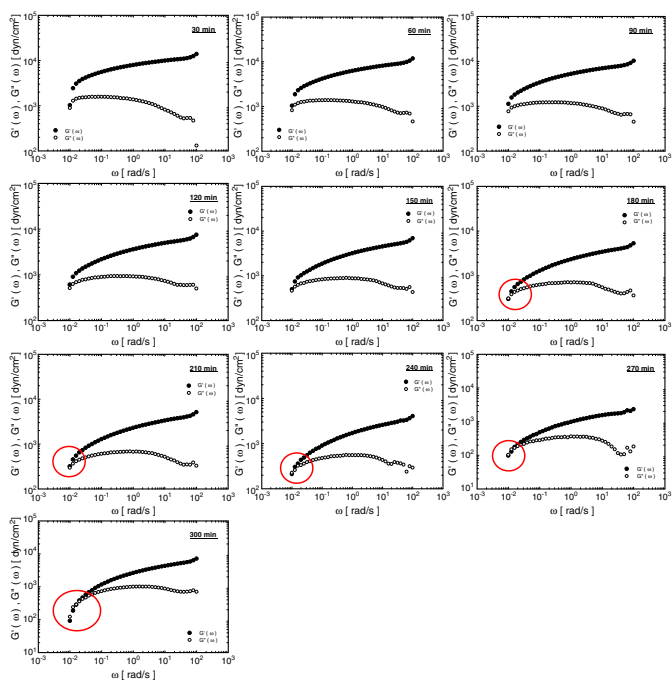


Fig. 4. Angular frequency dependencies of the dynamic moduli using the Advanced Rheometric Expansion system. The solid and open symbols represent the elastic modulus (the storage modulus: G') and the viscous modulus (the loss modulus: G'') for the barrier-layer, respectively. The red round symbols represent the contact regions of G' and G'' . (For interpretation of the references to color in this figure legend, the reader is referred to the web version of this article.)

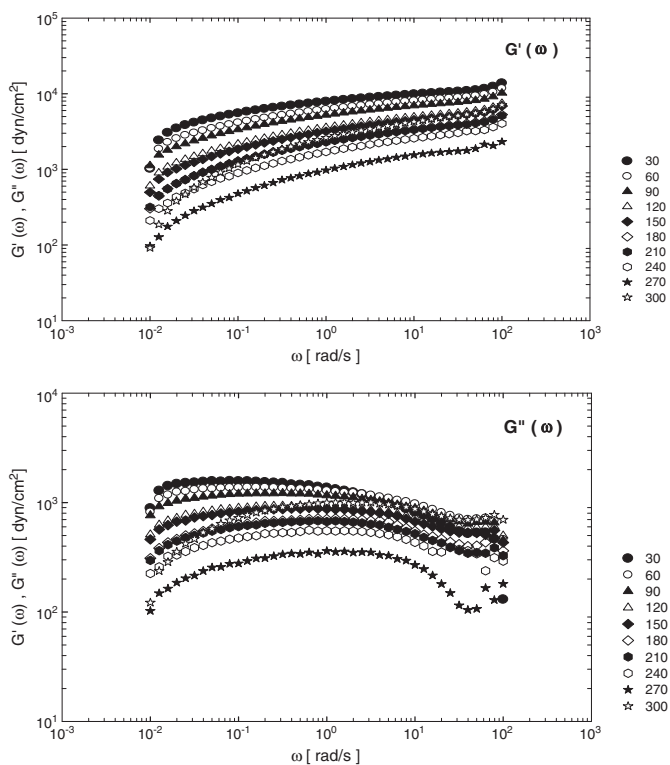


Fig. 5. Angular frequency dependencies of the dynamic moduli for the time intervals and the elastic modulus G' and viscous modulus G'' . Symbols represent the sampling time points (30, 60, 90, 120, 150, 180, 210, 240, 270, and 300 min).

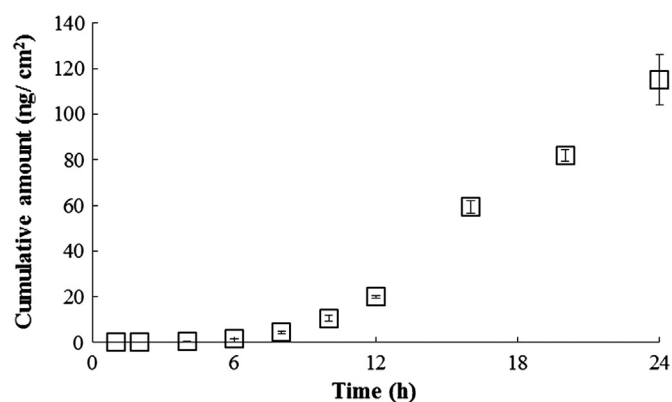


Fig. 6. *In vitro* drug diffusion profiles through the swollen barrier layer using side-by-side diffusion cells to achieve its lag time and diffusion coefficient ($n = 4$).

3.5. *In vitro* drug release profiles

The test tablets showed sigmoidal-type drug release profiles (Fig. 7a). The drug release rate decreased sharply after the initial high rate for 1 h, increased from 2 to 6 h, and then decreased again after 6 h (Fig. 7b). The drug release profiles might be divided into three stages according to the geometric characteristics of the test tablet and the drug release profiles. For the first stage (about 1 h in duration), drug release can take place on the surface of the mid-layer, as long as the mid-layer is not completely covered by the swollen barrier layer

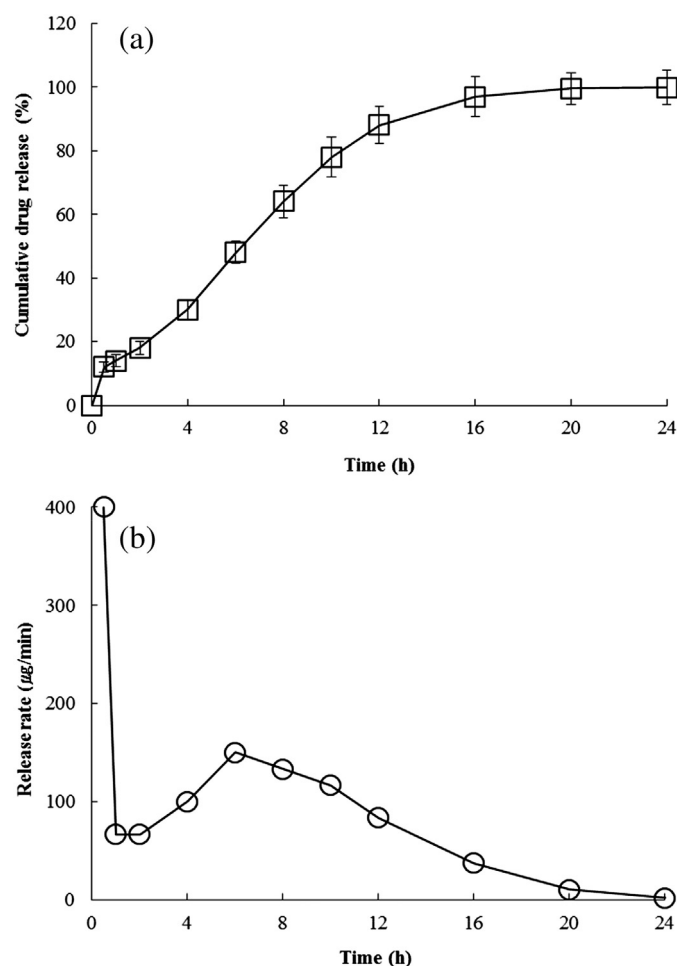


Fig. 7. Evaluation of *in vitro* drug release. (a) Drug release profiles and (b) drug release rates of the test tablets ($n = 4$).

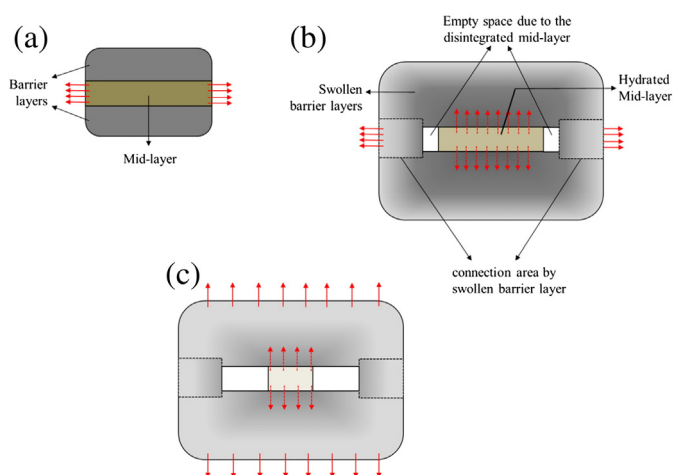


Fig. 8. Schematic view of the drug diffusion stages in the test tablet during the dissolution test. (a) The first stage as the mid-layer was not completely covered by the swollen barrier layer. (b) The second stage as the mid-layer was completely wrapped by the swollen barrier layer. (c) The last stage as the drug release from the mid-layer to the barrier layer was mainly controlled by the diffusion and erosion of the barrier layer.

(Fig. 8a). In the second stage (from 1 to 6 h), the mid-layer was completely wrapped by the swollen barrier layer. The dissolved drug in the mid-layer moved to the barrier layer and the contact regions of the swollen barrier layer (Fig. 8b). In the last stage (after 6 h), the drug release from the mid-layer to the barrier layer was mainly controlled by the diffusion and erosion of the barrier layer (Fig. 8c).

For the initial stage, the drug release profiles can be explained by the disintegration kinetics of the mid-layer. The mid-layer consisting of highly water-soluble excipients quickly disintegrated and dissolved. Therefore, the drug was rapidly released from the disintegrated mid-layer. At the same time, the aqueous medium penetrated easily leading to continuous disintegration of the layer. At the second stage, the dissolved drug in the mid-layer moved to the barrier layer and the contact region of the swollen barrier layer with the penetrated aqueous medium in the layer. The binding force between the polymers in the barrier layer may be larger than the force of the lateral contact region. The contact region of the swollen barrier layer had swollen already with more relaxation of the polymer chains, and so might erode faster than the barrier layer. On the other hand, the polymer in the barrier layer progressively swells [22,50]. The empty space comprising the disintegrated mid-layer during the initial stage was formed between the mid-layer and the contact region, which blocked the migration of the drug toward the contact region. Therefore, the drug was mainly released through the contact region exposed to the release medium during the second stage.

At the last stage, the release mechanisms were enacted by polymer swelling, polymer erosion/degradation, and diffusion. The drug migrating from the mid-layer to the barrier layer was released through the barrier layer. Thus, the properties of the polymer in the barrier layer were an important factor in the control of drug release at the last stage. Generally, the properties of the polymer dictate the relaxation of the polymer chains and aqueous medium absorption. The aqueous medium penetrates into the barrier layer and begins to modify the characteristics of the swelling gel, which becomes thicker due to the enlargement of the polymer chains [51]. As the thickness of the barrier layer was changed with the absorption of aqueous medium, the distance to release it out of the barrier layer was also increased. This increase of the distance had an effect on the drug release rate. The barrier layer began to erode as more aqueous medium came into the test tablet, and the barrier layer became thinner [52].

3.6. Imaging of *in vitro* drug release profiles using Raman spectroscopy

Based on the *in vitro* drug release profiles, three points were selected for the Raman spectroscopy at predetermined times (1 h, 3 h, and 5 h).

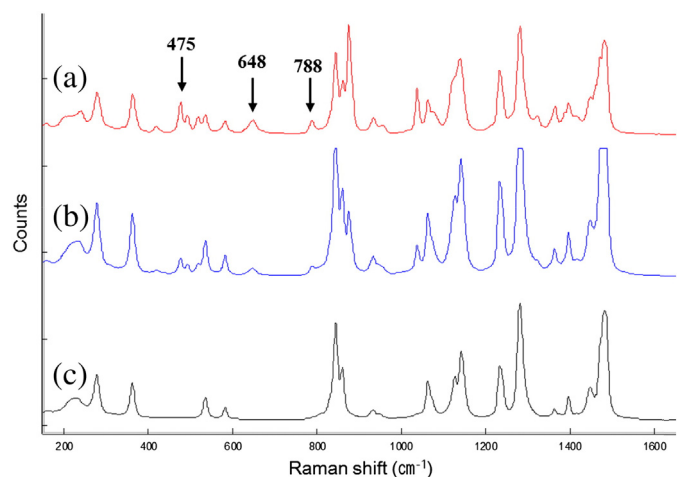


Fig. 9. Raman spectra analysis to distinguish intensive bands of the model drug. (a) Representative spectrum of the model drug. (b) Spectrum of the mid-layer measured at 1 h during the experiment. (c) Barrier layer surface before the experiment. The arrows indicate the bands used for determination of the drug.

Fig. 9 depicts the characteristic vibrational bands of the model drug. The spectrum of tamsulosin HCl showed three distinguishing intensive bands of 788 cm^{-1} , 648 cm^{-1} , and 475 cm^{-1} . The spectra were measured for the model drug itself (a), the mid-layer was measured at 1 h during the experiment (b), and the drug-free barrier layer surface before the experiment (c). Comparison of the Raman spectra of the samples revealed that, except for the above three vibrational bands, there were no distinguishable vibrational bands. Therefore, imaging was performed with an emphasis on these three bands.

Fig. 10 shows Raman imaging of the three different regions with the hydrated test tablet at 1 h, 3 h, and 5 h. The Raman shift region from 800 cm^{-1} to 470 cm^{-1} was used and emphasized in the software. The red color denoted the higher drug concentration compared to yellow, green, and blue. The imaging results were consistent with the pathways of drug migration in the drug release profiles. The dissolved drug in the mid-layer at 1 h began to move to the barrier layer and the contact regions of the swollen barrier layer. The concentration of the drug that had moved from the mid-layer to the barrier layer and the contact region had gradually increased at 3 h. Moreover, the moved drug at the contact region did not consistently accumulate, but was gradually released, whereas the drug accumulated at the barrier layer and was released after 5 h.

Fig. 10a depicts the swollen barrier layer in the area neighboring the surface. The drug moved from the mid-layer to the barrier layer at the initial 1 h mark, despite its very low concentration. However, a large amount of the drug moved to the barrier layer and it consistently accumulated at 3 h. This suggests that the dissolved drug in the mid-layer consistently migrated to the barrier layer. On the other hand, due to the continuous increase of the barrier layer's thickness and the coherence of the polymer chains, the drug that had moved to the barrier layer at 3 h was not sufficiently released. After the erosion/degradation of the swollen barrier layer began according to the relaxation of the polymer chains, the drug that accumulated in the barrier layer was released through the wide spaces between the polymers. Therefore, the color intensity at 5 h was completely faded compared to 3 h.

The distribution and movement of the drug at the contact region of the barrier layer with the mid-layer are depicted in **Fig. 10b**. At 1 h, the drug was mainly distributed in the mid-layer and was evenly distributed between the mid-layer and the barrier layer after 3 h. The drug in the mid-layer likely moved to the barrier layer due to the disintegration of the mid-layer. The disintegration resulted in a dappled

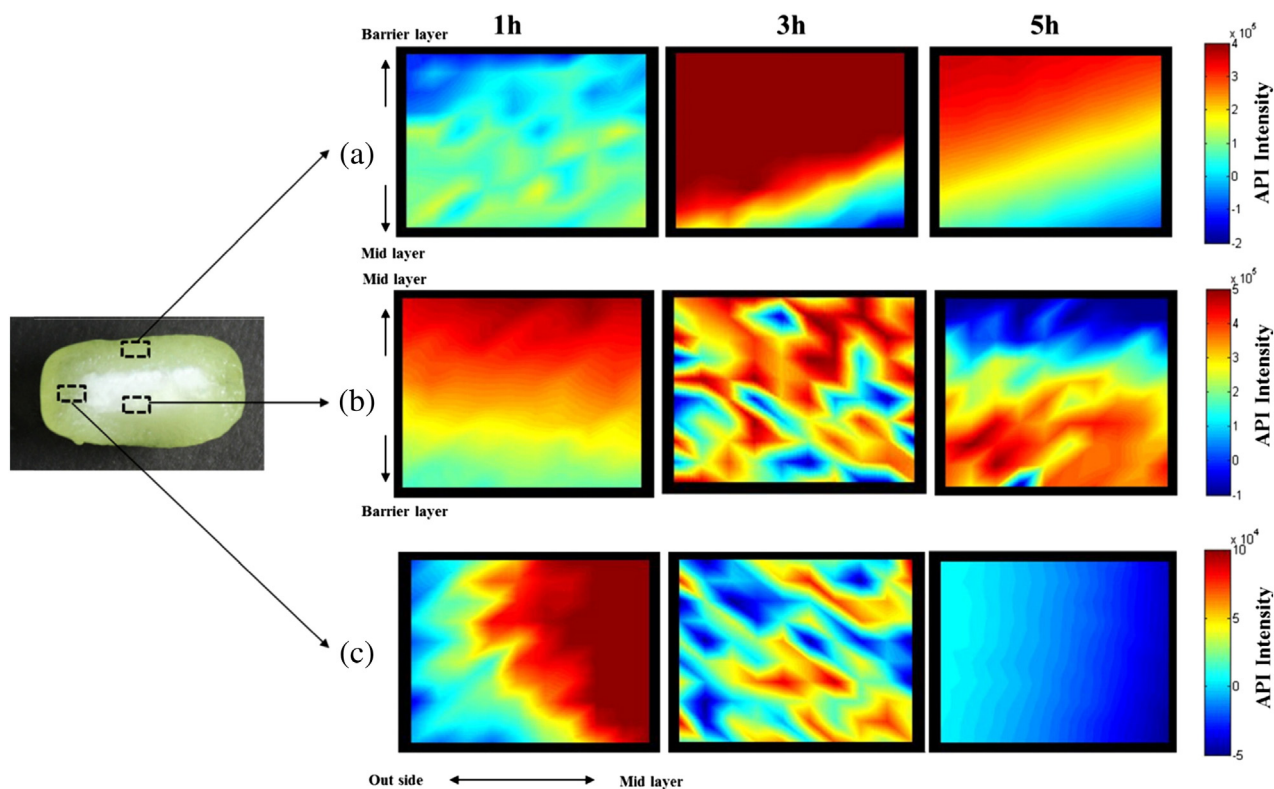


Fig. 10. Raman spectroscopy imaging of the three different regions of the hydrated test tablet. Representative spectra of (a) the swollen barrier layer neighboring the surface, (b) contact part of the barrier layer with the mid-layer, and (c) contact region of the swollen barrier layer neighboring the mid-layer. (For interpretation of the references to color in this figure, the reader is referred to the web version of this article.)

Table 2
Pharmacokinetic parameters of the geometric three-layered tablet.

$t_{1/2}^a$ (h)	T_{max} (h)	C_{max}^b (h)	AUC_{last}^a (h·ng/mL)	AUC_{inf}^a (h·ng/mL)	CL/F (L/h)
11.01 ± 3.50	7.70 ± 1.75	7.74 ± 2.46	153.43 ± 58.66	166.68 ± 69.22	2.86 ± 1.29

^a Calculated from mean plasma concentrations.

^b Geometric mean values.

pattern of distribution of the drug, not evenly dispersed. After 5 h, the concentration of the drug in the barrier layer increased more than in the mid-layer, so the area of the barrier layer was expressed as red, while the area of the mid-layer was evident in blue.

Fig. 10c shows a contact region of the swollen barrier layer neighboring the mid-layer. At 1 h, the concentration of the mid-layer was higher than that of the contact region. At 3 h, the drug had moved from the mid-layer to the contact region. The distribution of the drug was again dappled due to the disintegration of the mid-layer. However, the drug migration was limited. The exposed surface of the mid-layer disintegrated during the initial stage, so an empty space was observed between the mid-layer and the contact region. Therefore, the drug did not move from the mid-layer to the contact region after a certain time, and the drug did not appear at the contact region after 5 h.

3.7. Pharmacokinetic analysis in humans

Evaluating the physical properties of test tablets and *in vitro* dissolution can clarify drug movement and release mechanisms. Previous studies confirmed that the drug could be absorbed in the large intestine and that it may present feasible formulations for once-a-day drug administration [30,53]. Therefore, an *in vivo* pharmacokinetic study using human volunteers was carried out to evaluate the pharmacokinetic profiles from the geometric mechanism.

Table 2 and Fig. 11 present the statistical summary for the pharmacokinetic data and mean plasma drug concentration profiles. Mean plasma concentrations throughout 48 h for the test tablet increased until 9 h and then gradually decreased after 10 h, while the mean plasma concentrations increased until 9 h in a sigmoid profile. It was significantly increased for the first 1 h, slightly increased from 2 to 3 h, and increased gradually from 4 to 6 h. This showed that the mean plasma concentrations and *in vitro* dissolution had similar profiles. Due to the geometric properties of the test tablet, the drug was released from the mid-layer for the first 1 h then the mid-layer was wrapped by the swollen barrier layers for 2–3 h. At this time, very little drug was released from the barrier layer that surrounded the mid-layer. After 4 h, the drug in the mid-layer moved with the absorbed medium to the barrier layers and it was gradually released into the dissolution medium. Moreover, the half-life, T_{max} , and C_{max} were 11.01 h, 7.70 h, and 7.74 h, respectively, indicating that the model drug from the swollen barrier layer after 4 h was continuously released and absorbed in plasma.

The absorption rate *in vivo* was calculated using the Wagner–Nelson equation and deconvolution of mean plasma concentration (Fig. 11b). Comparing the *in vitro* dissolutions demonstrated a similar profile of the total extent of *in vivo* absorption from the test tablet. As mentioned already, the two profiles displayed an initial rapid absorption of about 10% of the total at 1 h. After that time, the rate of absorption was decreased until 3 h and then the rate was increased about 50% of the total absorption until 6 h. However, the *in vivo* fractional absorption rate was not comparable to the *in vitro* dissolution due to the half-life (11.01 h) and clearance rate (2.86 L/h). This result suggested that the *in vitro* dissolution profiles and *in vivo* plasma drug concentration–time profiles showed similar profiles showing decent geometric properties.

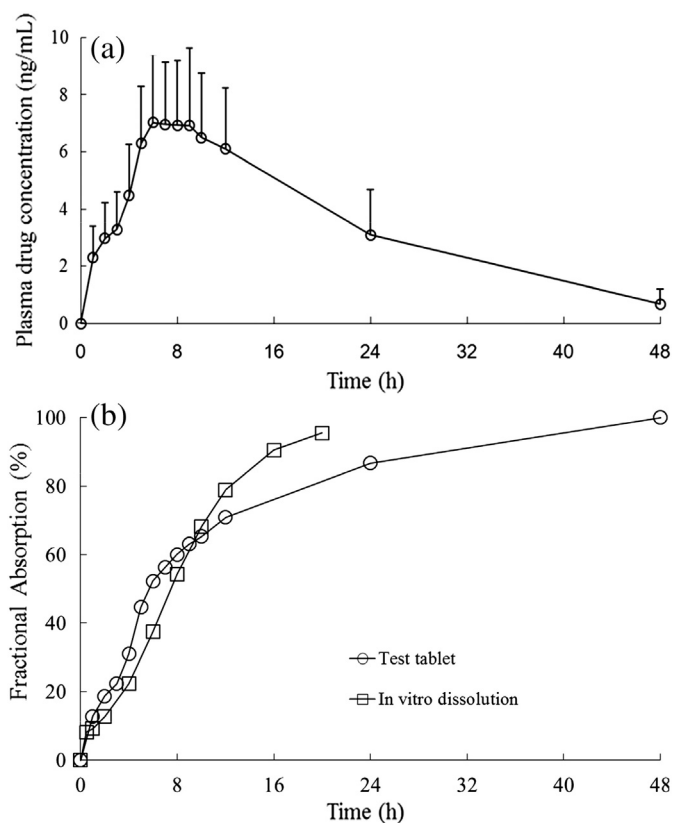


Fig. 11. (a) Pharmacokinetic profile of the test tablet in humans ($n = 27$) and (b) *in vitro* dissolution and *in vivo* drug absorption for the test tablet after deconvolution of plasma drug concentration–time profiles according to the Wagner–Nelson method.

4. Conclusions

Using the physical properties of the matrix tablets, the geometric three-layered tablets were evaluated to trace the drug migration in the tablet and to better understand the correlation between geometric properties and *in vitro/in vivo* drug release. The test tablets were quickly permeated by the aqueous medium and rapidly swelled to form gelled layers surrounding the surface of the mid-layer, which produced controlled drug release profiles. The thickness of the gelled layers was increased with continuous aqueous medium absorption, relaxing the polymer chains gradually. A sigmoidal type of drug release was observed and could be modified to release the incorporated drug for a longer period of time. It could also overcome the initial burst effect or dose dumping of a common matrix tablet by incorporating drugs mainly in the mid-layer than in the barrier layers. Raman spectroscopy mapping indicated the pathway of the drug in the geometric tablet and these results corresponded well with the drug release profiles. The pharmacokinetic study indicated that *in vitro* dissolution profiles and *in vivo* plasma absorption concentrations had similar sigmoid types of drug release due to the geometric properties of the test tablet. These results provide valuable information for the understanding of the geometric dose system, especially using hydrophilic polymers.

Acknowledgments

This research was supported by the Basic Science Research Program through the National Research Foundation of Korea (NRF) funded by the Ministry of Education, Science and Technology (2012002399) and by a grant of the Korean Health Technology R&D Project, Ministry for Health, Welfare & Family Affairs, Republic of Korea (A092018).

References

- [1] Y.V.R. Prasad, Y.S.R. Krishnaiah, S. Satyanarayana, *In vitro* evaluation of guar gum as a carrier for colon-specific drug delivery, *J. Control. Release* 51 (1998) 281–287.
- [2] U. Conte, L. Maggi, P. Colombo, A. La Manna, Multi-layered hydrophilic matrices as constant release devices (Geomatrix™ Systems), *J. Control. Release* 26 (1993) 39–47.
- [3] S. Sershen, J. West, Implantable, polymeric systems for modulated drug delivery, *Adv. Drug Deliv. Rev.* 54 (2002) 1225–1235.
- [4] T.F. Vandamme, K.J. Ellis, Issues and challenges in developing ruminal drug delivery systems, *Adv. Drug Deliv. Rev.* 56 (2004) 1415–1436.
- [5] C.G. Varelas, D.G. Dixon, C.A. Steiner, Zero-order release from biphasic polymer hydrogels, *J. Control. Release* 34 (1995) 185–192.
- [6] Y. Qiu, N. Chidambaram, K. Flood, Design and evaluation of layered diffusional matrices for zero-order sustained-release, *J. Control. Release* 51 (1998) 123–130.
- [7] V. Pillay, R. Fassihi, Electrolyte-induced compositional heterogeneity: a novel approach for rate-controlled oral drug delivery, *J. Pharm. Sci.* 88 (1999) 1140–1148.
- [8] S. Andjelić, J. Yuan, D. Jamiolkowski, R. Diluccio, R. Bezwada, H. Zhang, J. Mijović, Hydrophilic absorbable copolyester exhibiting zero-order drug release, *Pharm. Res.* 23 (2006) 821–834.
- [9] S.X. Wang, A. Bao, W.T. Phillips, B. Goins, S.J. Herrera, C. Santoyo, F.R. Miller, R.A. Otto, Intraoperative therapy with liposomal drug delivery: retention and distribution in human head and neck squamous cell carcinoma xenograft model, *Int. J. Pharm.* 373 (2009) 156–164.
- [10] J. Siepmann, A. Göpferich, Mathematical modeling of bioerodible, polymeric drug delivery systems, *Adv. Drug Deliv. Rev.* 48 (2001) 229–247.
- [11] J. Siepmann, N. Peppas, Modeling of drug release from delivery systems based on hydroxypropyl methylcellulose (HPMC), *Adv. Drug Deliv. Rev.* 48 (2001) 139–157.
- [12] P.I. Lee, Kinetics of drug release from hydrogel matrices, *J. Control. Release* 2 (1985) 277–288.
- [13] N.A. Peppas, J.J. Sahlin, A simple equation for the description of solute release. III. Coupling of diffusion and relaxation, *Int. J. Pharm.* 57 (1989) 169–172.
- [14] U. Conte, L. Maggi, A flexible technology for the linear, pulsatile and delayed release of drugs, allowing for easy accommodation of difficult *in vitro* targets, *J. Control. Release* 64 (2000) 263.
- [15] B. Narasimhan, R. Langer, Zero-order release of micro- and macromolecules from polymeric devices: the role of the burst effect, *J. Control. Release* 47 (1997) 13–20.
- [16] P. Hildgen, J.N. McMullen, A new gradient matrix: formulation and characterization, *J. Control. Release* 34 (1995) 263–271.
- [17] M.P. Danckwerts, Development of a zero-order release oral compressed tablet with potential for commercial tableting production, *Int. J. Pharm.* 112 (1994) 37–45.
- [18] A.Y. Benkorah, J.-N. McMullen, Biconcave coated, centrally perforated tablets for oral controlled drug delivery, *J. Control. Release* 32 (1994) 155–160.
- [19] A.C. Shah, N.J. Britten, Novel divisible tablet designs for sustained release formulations, *J. Control. Release* 14 (1990) 179–185.
- [20] P. Colombo, U. Conte, A. Gazzaniga, L. Maggi, M.E. Sangalli, N.A. Peppas, A. La Manna, Drug release modulation by physical restrictions of matrix swelling, *Int. J. Pharm.* 63 (1990) 43–48.
- [21] U. Conte, L. Maggi, M.L. Torre, P. Giunchedi, A.L. Manna, Press-coated tablets for time-programmed release of drugs, *Biomaterials* 14 (1993) 1017–1023.
- [22] C. Maderuelo, A. Zarzuelo, J.M. Lanao, Critical factors in the release of drugs from sustained release hydrophilic matrices, *J. Control. Release* 154 (2011) 2–19.
- [23] A.S. El-Hagrasy, F. D'Amico, J.K. Drennen, A Process Analytical Technology approach to near-infrared process control of pharmaceutical powder blending. Part I: D-optimal design for characterization of powder mixing and preliminary spectral data evaluation, *J. Pharm. Sci.* 95 (2006) 392–406.
- [24] A.S. El-Hagrasy, M. Delgado-Lopez, J.K. Drennen, A Process Analytical Technology approach to near-infrared process control of pharmaceutical powder blending: part II: qualitative near-infrared models for prediction of blend homogeneity, *J. Pharm. Sci.* 95 (2006) 407–421.
- [25] A.S. El-Hagrasy, J.K. Drennen, A Process Analytical Technology approach to near-infrared process control of pharmaceutical powder blending. Part III: quantitative near-infrared calibration for prediction of blend homogeneity and characterization of powder mixing kinetics, *J. Pharm. Sci.* 95 (2006) 422–434.
- [26] M. Andersson, S. Folestad, J. Gottfries, M.O. Johansson, M. Josefson, K.-G. Wahlund, Quantitative analysis of film coating in a fluidized bed process by in-line NIR spectrometry and multivariate batch calibration, *Anal. Chem.* 72 (2000) 2099–2108.
- [27] D.A. Long, *The Raman Effect: A Unified Treatment of the Theory of Raman Scattering by Molecules*, John Wiley and Sons, New York, 2002.
- [28] E. Smith, G. Dent, J. Wiley, *Modern Raman Spectroscopy: a Practical Approach*, John Wiley and Sons, New York, 2005.
- [29] K.C. Gordon, C.M. McGovern, Raman mapping of pharmaceuticals, *Int. J. Pharm.* 417 (2011) 151–162.
- [30] J.S. Park, J.Y. Shim, J.S. Park, Y.W. Choi, S.H. Jeong, A novel three-layered tablet for extended release with various layer formulations and *in vitro* release profiles, *Drug Dev. Ind. Pharm.* 37 (2011) 664–672.
- [31] S. Jamzad, L. Tutunji, R. Fassihi, Analysis of macromolecular changes and drug release from hydrophilic matrix systems, *Int. J. Pharm.* 292 (2005) 75–85.
- [32] H. Li, X. Gu, Correlation between drug dissolution and polymer hydration: a study using texture analysis, *Int. J. Pharm.* 342 (2007) 18–25.
- [33] S. Nazzal, M. Nazzal, Y. El-Malah, A novel texture-probe for the simultaneous and real-time measurement of swelling and erosion rates of matrix tablets, *Int. J. Pharm.* 330 (2007) 195–198.
- [34] V. Pillay, R. Fassihi, A novel approach for constant rate delivery of highly soluble bioactives from a simple monolithic system, *J. Control. Release* 67 (2000) 67–78.
- [35] R. Taylor, R. Krishna, *Multicomponent Mass Transfer*, John Wiley and Sons, New York, 1993.
- [36] F.C. Collins, G.E. Kimball, Diffusion-controlled reaction rates, *J. Colloid Sci.* 4 (1949) 425–437.
- [37] J. Müller, D. Brock, K. Knop, J. Axel Zeitler, P. Kleinebudde, Prediction of dissolution time and coating thickness of sustained release formulations using Raman spectroscopy and terahertz pulsed imaging, *Eur. J. Pharm. Biopharm.* 80 (2012) 690–697.
- [38] M. Kim, H. Chung, Y. Woo, M. Kemper, New reliable Raman collection system using the wide area illumination (WAI) scheme combined with the synchronous intensity correction standard for the analysis of pharmaceutical tablets, *Anal. Chim. Acta* 579 (2006) 209–216.
- [39] T. Sawada, K. Sako, M. Fukui, S. Yokohama, M. Hayashi, A new index, the core erosion ratio, of compression-coated timed-release tablets predicts the bioavailability of acetaminophen, *Int. J. Pharm.* 265 (2003) 55–63.
- [40] K. Rao, K.P. Devi, P. Buri, Influence of molecular size and water solubility of the solute on its release from swelling and erosion controlled polymeric matrices, *J. Control. Release* 12 (1990) 133–141.
- [41] K. Mitchell, J. Ford, D. Armstrong, P. Elliott, J. Hogan, C. Rostron, The influence of drugs on the properties of gels and swelling characteristics of matrices containing methylcellulose or hydroxypropylmethylcellulose, *Int. J. Pharm.* 100 (1993) 165–173.
- [42] L.S.C. Wan, P.W.S. Heng, L.F. Wong, Relationship between swelling and drug release in a hydrophilic matrix, *Drug Dev. Ind. Pharm.* 19 (1993) 1201–1210.
- [43] C. Caramella, F. Ferrari, M. Bonferoni, M. Ronchi, P. Colombo, Rheological properties and diffusion dissolution behaviour of hydrophilic polymers, *Boll. Chim. Farm.* 128 (1989) 298.
- [44] V.S. Rudraraju, C.M. Wyandt, Rheology of microcrystalline cellulose and sodiumcarboxymethyl cellulose hydrogels using a controlled stress rheometer: part II, *Int. J. Pharm.* 292 (2005) 63–73.
- [45] H. Suwardi, P. Wang, D.B. Todd, V. Panchal, M. Yang, C.G. Gogos, Rheological study of the mixture of acetaminophen and polyethylene oxide for hot-melt extrusion application, *Eur. J. Pharm. Biopharm.* 78 (2011) 506–512.
- [46] J.S. Park, J.Y. Shim, N.K.V. Truong, J.S. Park, S. Shin, Y.W. Choi, J. Lee, J.-H. Yoon, S.H. Jeong, A pharma-robust design method to investigate the effect of PEG and PEO on matrix tablets, *Int. J. Pharm.* 393 (2010) 80–88.
- [47] N.A. Peppas, R. Gurny, E. Doelker, P. Buri, Modelling of drug diffusion through swellable polymeric systems, *J. Membr. Sci.* 7 (1980) 241–253.
- [48] R.T.C. Ju, P.R. Nixon, M.V. Patel, Drug release from hydrophilic matrices. 1. New scaling laws for predicting polymer and drug release based on the polymer disentanglement concentration and the diffusion layer, *J. Pharm. Sci.* 84 (1995) 1455–1463.
- [49] R.T.C. Ju, P.R. Nixon, M.V. Patel, D.M. Tong, Drug release from hydrophilic matrices. 2. A mathematical model based on the polymer disentanglement concentration and the diffusion layer, *J. Pharm. Sci.* 84 (1995) 1464–1477.
- [50] L. Maggi, L. Segale, M. Torre, E. Ochoa Machiste, U. Conte, Dissolution behaviour of hydrophilic matrix tablets containing two different polyethylene oxides (PEOs) for the controlled release of a water-soluble drug. Dimensionality study, *Biomaterials* 23 (2002) 1113–1119.
- [51] A. Pham, P. Lee, Probing the mechanisms of drug release from hydroxypropylmethyl cellulose matrices, *Pharm. Res.* 11 (1994) 1379–1384.
- [52] P. Colombo, R. Bettini, P. Santi, N.A. Peppas, Swellable matrices for controlled drug delivery: gel-layer behaviour, mechanisms and optimal performance, *Pharm. Sci. Technol. Today* 3 (2000) 198–204.
- [53] J.S. Park, J.Y. Shim, J.S. Park, M.J. Lee, J.M. Kang, S.H. Lee, M.C. Kwon, Y.W. Choi, S.H. Jeong, Formulation variation and *in vitro-in vivo* correlation for a rapidly swellable three-layered tablet of tamsulosin HCl, *Chem. Pharm. Bull.* 59 (2011) 529–535.